ELSEVIER

Physica B 244 (1998) 96–102

PHYSICA B

Vibrational properties of the CDW condensate in the quasi-one-dimensional conductor $(TaSe_4)_2I$: Numerical and experimental study

V.M. Burlakov[a,*], M.A. Moskalenko[a], D. Berner[b], H.P. Geserich[b], A. Zibold[c], D.B. Tanner[c], F. Lévy[d], H. Berger[d]

[a] *Institute of Spectroscopy Russian Academy of Sciences, 142092 Troitsk, Moscow region, Russian Federation*
[b] *Institut für Angewandte Physik, Universität Karlsruhe D-76128 Karlsruhe, Germany*
[c] *Department of Physics, University of Florida, Gainesville, FL 32611, USA*
[d] *Institut de Physique Appliquée, EPF de Lausanne, PHB Ecublens, 1015 Lausanne, Switzerland*

Abstract

We report on the numerical and experimental study of the vibrational spectrum of the charge-density-wave (CDW) conductor $(TaSe_4)_2I$. The microscopic mechanism accounting for the giant IR peak at frequencies about $\sim 40\ cm^{-1}$ in the $(TaSe_4)_2I$ is proposed. The mechanism is based on an assumption about dynamical charge transfer between adjacent CDW periods accompanying their vibration in corresponding normal mode with wave vector equal to that of superstructure. The mechanism is consistent also with the increase in the IR intensity of the peak observed experimentally when heating the $(TaSe_4)_2I$ crystal above the Peierls transition temperature $T_p = 261$ K. Critical index of the Peierls transition order parameter determined from the temperature dependence of the phase phonons intensity is found to be about 0.17, consistent with the results of X-ray experiments.

Keywords: $(TaSe_4)_2I$; Charge-density waves

1. Introduction

Vibrational and transport properties of quasi-1-D conductors in the Peierls–Fröhlich state attract great interest due to numerous peculiarities. The most striking among them are: (i) the giant peak of unknown origin in the low-frequency IR spectrum of a number of inorganic charge-density wave (CDW) conductors such as $K_{0.3}MoO_3$, $(TaSe_4)_2I$ and TaS_3 [1–3]; (ii) nonlinear conductivity and noise generation when conducting DC current by these materials. It is suggested that this phenomenon can be ascribed to an influence of defects. Present communication is devoted to analytical and numerical study of vibrational properties of a model system, which obey all the above-mentioned intrinsic features of CDW conductors in the Peierls–Fröhlich state. We believe that after comparison of the numerical results with the experimental data and proper justification of the model it can serve as a bases for understanding of the microscopic nature of the above-peculiar features.

* Corresponding author.

0921-4526/98/$19.00
PII S0921-4526(97)00469-9

The low-frequency excitation spectrum of the CDW ground state have been widely investigated both theoretically and experimentally (see, e.g., reviews [4–6] and references therein). It is well established that incommensurate CDW ground state is characterized by two specific collective excitations: IR active phase mode and Raman active amplitude mode [7]. The frequency of the former, ω_p, in the incommensurate CDW conductors is of the order of $1\,cm^{-1}$ while the amplitude mode frequency ω_a is about one–two orders of magnitude higher. These vibrations have been observed experimentally in such model CDW conductors as $K_{0.3}MoO_3$, $(TaSe_4)_2I$ and TaS_3 [1, 2, 8–14].

Besides the phase and the amplitude modes an additional vibration obeying giant IR activity has been observed in all the above-mentioned compounds [1–3]. The frequency of this additional feature in $(TaSe_4)_2I$ is about $38\,cm^{-1}$ in between the phase ($\sim 1\,cm^{-1}$, Ref. [13]) and the amplitude ($\sim 90\,cm^{-1}$, Ref. [10]) mode frequencies. Several explanations have been proposed to account for the additional giant IR peak, but microscopic origin of this vibration is still not clear (see, for instance, the discussions in Refs. [1, 15]). An interesting phenomenological model has been proposed by Degiorgi and Grüner [15] although the microscopic origin of some phenomenological parameters of this model remains unclear. According to this model, the additional IR peak results from a bound collective-mode resonance localized around impurity.

In the present study, it is shown that the giant IR resonance occurs in the incommensurate CDW system even in the absence of any impurities provided that the dynamical charge transfer between adjacent CDW periods is taken into account. For description of vibrational and transport properties of CDW system a model system of interacting particles in sinusoidal external potential (Frenkel–Kontorova (FK) model [16]) has been used. The theoretical vibrational spectra have been compared with those obtained experimentally for $(TaSe_4)_2I$ CDW conductor.

The theoretical investigations have been performed in two approaches: (i) molecular dynamic (MD) simulation has been used for the system to reach an equilibrium state according to the method proposed in Ref. [17], after what all the particles has been subjected to a small uniform step-like displacement and subsequent vibrations has been analyzed via Fourier transformation; (ii) eigenvector problem (EVP) has been solved in the harmonic approximation to study the vibrational spectrum of the system. The superstructure in this case has been taken into account through expansion of the potential energy around particle equilibrium positions determined from MD simulation.

Experimental IR conductivity was calculated via Kramers–Kronig transformation of IR reflectance spectra measured at near-normal incidence by means of Michelson interferometer ($6–100\,cm^{-1}$) and with Bruker 113v Fourier-transform spectrometer (80 and $22\,000\,cm^{-1}$).

2. Results and discussion

2.1. Model description and numerical results

Since the lattice deformation coupled to the CDW is much smaller than the crystal-lattice constant, it is reasonable to describe the CDW system within the FK model. Let us consider a chain of particles of mass m and charge e with nearest-neighbor Column interaction in the sinusoidal external (crystal lattice) potential

$$V(x) = -(Va^2/4\pi^2)\cos(2\pi x/a).$$

Motion equation for nth particle is

$$m\frac{\partial^2 U_n}{\partial t^2} + \gamma\frac{\partial U_n}{\partial t} + K_2 a^3\left[\frac{e^2}{(U_{n+1}-U_n)^2} - \frac{e^2}{(U_n-U_{n-1})^2}\right] + \frac{Va}{2\pi}\sin\left(2\pi\frac{U_n}{a}\right) = eE(t), \quad (1)$$

where γ is phenomenological damping and $E(t)$ is the external electric field. We will consider the interparticle distance in the phase without superstructure to be equal to $2a$ which means the CDW is formed due to dimerization. In case if the number of particles differs from the half-number of the potential minima one obtains superstructure. Then the time-dependent position U_n of the particle can be represented as $U_n = 2na + U_n^0 + \delta_n(t)$, where

U_n^0 is quasi-static variable describing a shift of the equilibrium position of the particle with respect to the corresponding potential minimum, $\delta_n(t)$ describes a vibration of the particle around the new equilibrium position U_n^0. In the harmonic approximation and suggesting $\delta_n(t) = \delta_n(\omega)\exp(i\omega t)$ and $E(t) = E_0 \cdot \exp(i\omega \cdot t)$ Eq. (1) can be reduced to two equations:

$$\tilde{K}_2(2U_n^0 - U_{n-1}^0 - U_{n-1}^0) + \frac{V}{2\pi}\sin(2\pi U_n^0) = 0 \quad (2)$$

and

$$\delta_n(\omega)[V\cos(2\pi U_n^0) - \omega^2 + i\omega\gamma] + \tilde{K}_2(2\delta_n(\omega) - \delta_{n-1}(\omega) - \delta_{n+1}(\omega)) = E_0 \quad (3)$$

suitable for analytical study. $\tilde{K}_2 = 2K_2e^2a^3/(b^3m) \simeq K_2/4$, where $b \simeq 2a$ is the average interparticle distance. Here and below we accepted $m = 1$, $e = 1$ and $a = 1$. Disregarding the trivial case $U_n^0 = 0$ Eq. (2) describes quasi-static kink-like deformation of the chain (due to neglection of the dynamical term we restrict our consideration by standing kinks only), while Eq. (3) describes the particle vibration around the new equilibrium position. In the continuous limit Eq. (2) reduces to the sine-Gordon equation [18–20] with the single-kink solution [21] $U_n^0(i) = 2\pi^{-1} \cdot \mathrm{arctg}\{\exp[\pm\frac{4(n-i)a}{R_k}]\}$, $R_k = 4\sqrt{(\tilde{K}_2/V)}$ can be considered as the kink radius measured in a units, i is the kink position. Although the N-kink solution U_n^0 of Eq. (3) is also available [22] it is more convenient to approximate it with the sum of the single-kink solutions $U_n^0 \simeq \sum U_n^0(i)$. Our MD study of the ground state of a system consisting of 128 particles arranged in $256 + N_k$ potential wells with cyclic boundary conditions showed that even for $N_k \gg 1$ (N_k is a number of kinks) the kink lattice or, in the other words, superstructure with the wavevector $k_s = \pi \cdot N_k/(128 \cdot b)$, can be perfectly described as a sum of the single-kink solutions with some effective R_k, although the latter looses its meaning as the kink radius when exceeding the half-period of the kink lattice (superstructure) [23].

Fig. 1a shows the fragment of MD simulation result for arrangement of 128 particles over 264 potential wells, thus we simulated CDW with

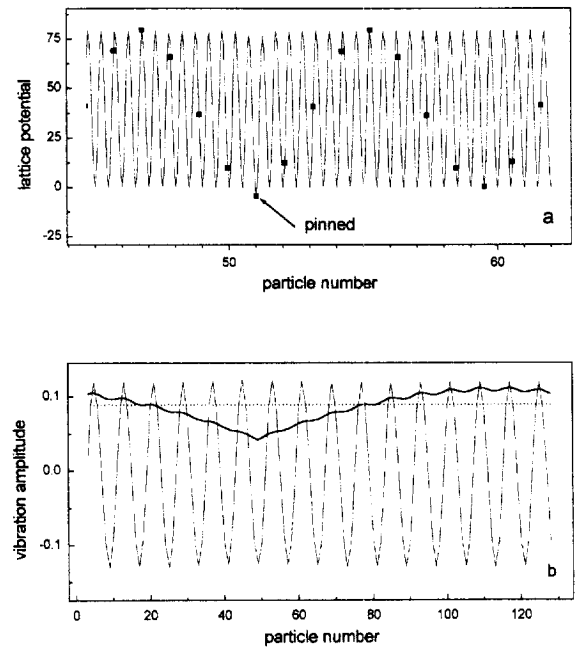

Fig. 1. (a) Fragment of particle arrangement obtained via MD simulation in the Frenkel–Kontorova model containing 128 particles arranged over 272 potential minima ($k_s = \frac{8}{9}\pi/b$) and subjected to circlic boundary conditions. The particle No. 51 is pinned by an extra local potential. (b) Eigenvectors of phason mode without pinning (dotted line) and with pinning (thick solid line), and those of CT mode (see Fig. 2) shown by thin solid line for both pinned and depinned chain.

superstructure period. The 51th particle (shown by arrow in the figure) is pinned. The conductivity spectra $I(\omega) = \omega \cdot \mathrm{Im}[(\sum\delta_n(\omega))/E_0]$ obtained from MD simulation are shown in Fig. 2 for both pinned and depinned system. The features of our interest are the phase mode (PM) and the peak CT mode (charge-transfer mode), marked by PM- and CT-arrows in Fig. 2, respectively. The latter peak of very weak intensity is genetically related to the vibration with the wavevector equal to that of the superstructure. The corresponding eigen vectors are shown in Fig. 1b. We will show that the CT peak acquires the giant IR intensity if one takes into account, the fact that the CDW internal deformation related to this vibration can be adiabatically accompanied by charge redistribution. As it has been demonstrated by Itkis and Brill [24], spatial redistribution of the charge condensed in

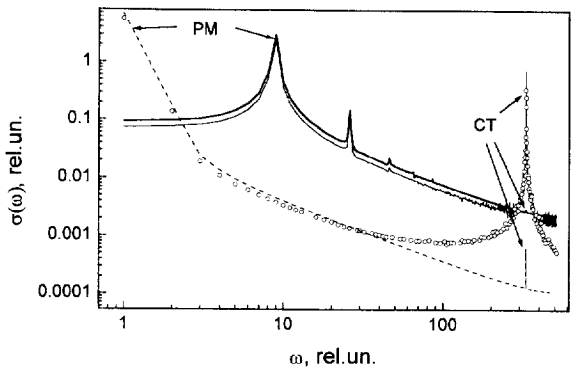

Fig. 2. Model IR conductivity spectra of the FK model (see caption to Fig. 1), calculated using Eqs. (3)–(5) for $4\sqrt{(\tilde{K}_2/V)} = 6$. Thin solid line is for $\beta = 0$ and thick solid line is for $\beta = 30$ in case of pinned chain. Dashed line is for $\beta = 0$ and symbols are for $\beta = 30$ in case of depinned chain. PM are the phase modes and CT are the modes which intensity may contain the charge-transfer contribution. For $\beta = 30$ the $0.03e$ of the particle charge is transferred during the CT mode vibration while for $\beta = 0$ it is 0.

CDW takes place under action of static electric field. Obviously, a characteristic time for the charge redistribution or, in the other words, for the charge transfer from one CDW period to the other is determined by the amplitude-mode frequency ($\sim 90\,\mathrm{cm}^{-1}$, Ref. [10]). Therefore, in the case of the CT vibration the adiabatic condition is fulfilled.

To take into account the charge transfer contribution to the IR intensity of any mode let us suppose that the particle charge in our model is determined as

$$\tilde{e}_n(t) = e(1 + \beta(\delta_{n+1}(t) - \delta_{n-1}(t))), \tag{4}$$

what means that the charge is transferred from the region of local compression of the CDW to a region of local dilatation. The factor β determines the fraction of the particle charge transferred during vibration. The dipole moment is determined as a sum of the part related to the particles displacement and the part, related to the charge transfer between adjacent unit cells

$$P(t) = \sum[e\delta_n(t) + e\beta\cdot(U_n^0 - U_{n-1}^0)(\delta_{n+1}(t) - \delta_{n-1}(t))]. \tag{5}$$

If we suppose, the charge variation to be of the order of $0.1e$ which means $\beta \sim 0.1/\delta_n^0$, where δ_n^0 is the vibration amplitude of particles in the corresponding phonon mode, then the charge-transfer effect will increase the total dipole moment roughly by factor $\sim 0.1e\cdot(U_n^0 - U_{n-1}^0)/\delta_n^0 \sim 10^2$. The conductivity spectra in which the charge-transfer effect has been taken into account according to Eq. (4) and Eq. (5) are shown in Fig. 2 by symbols (depinned chain) and thin solid line (pinned chain). The phase mode intensity remains nearly the same while the CT mode intensity increases several orders in magnitude. This occurs due to coincidence between the wave vector of the CT mode on the one hand and the superstructure wave vector on the other. Fig. 3 shows that the CT mode intensity ($\mathrm{Im}[(\sum\delta_n(\omega)/E_0)]$) included charge-transfer contribution possess a universal dependence on the parameter $4\sqrt{(\tilde{K}_2/V)}$ regardless the superstructure wave vector, while the intensity without charge-transfer contribution strongly depend on the superstructure wave vector and possess another universality [23].

2.2. Experimental conductivity spectra

Fig. 4 shows the room temperature and 10 K conductivity spectra for polarization along the chains. As it can be seen from the figure, the two basic changes in the spectrum take place upon cooling: (i) an appearance of the pronounced feature representing the Peierls energy gap at frequencies around 500 meV; (ii) a development of sharp structure in the low-frequency range. The low-frequency spectrum is quite similar to that obtained by Sherwin et al. [11].

The structure below 50 meV is a matter of our present study while the temperature-dependent conductivity around the Peierls gap value will be discussed elsewhere.

The giant low-frequency peak in the 10 K spectrum in Fig. 4 with intensity approaching 10 000 S and frequency about $38\,\mathrm{cm}^{-1}$ is that in which origin is discussed and we assign it to the CT mode. The sharp structure above this peak should be assigned to the so-called phase phonons [25, 26].

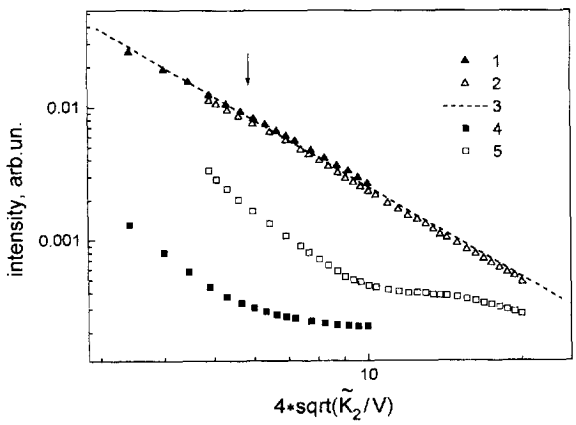

Fig. 3. Dependence of the CT mode integrated intensity on the potential parameters of the FK model containing 128 particles arranged over 264 minima ($k_s = \frac{1}{16}\pi/b$): (1) is for $\beta = 30$ and (4) is for $\beta = 0$; over 272 minima ($k_s = \frac{1}{18}\pi/b$): (2) is for $\beta = 30$ and (5) is for $\beta = 0$. (3) is the dependence $y = 0.45/x^{2.25}$. Arrow shows the parameters for the spectra presented in Fig. 2.

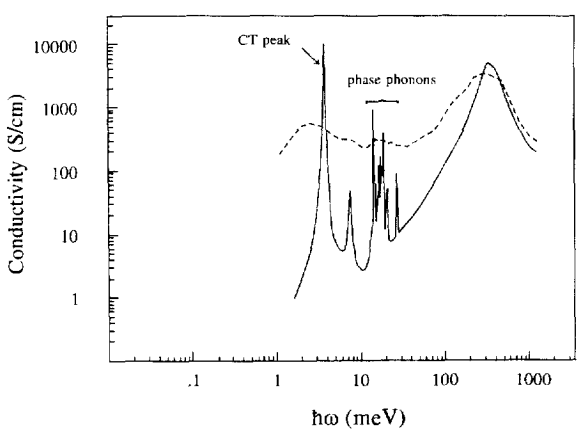

Fig. 4. Optical conductivity spectra of $(TaSe_4)_2I$ single crystal for $E \| c$ at room temperature (dashed line) and 10 K (solid line) calculated via Drude–Lorenz fit from corresponding reflectivity spectra.

These are totally symmetric vibrations participating in the stabilization of the CDW. Their IR activity results from small-amplitude phase vibrations of partial charge densities with respect to the total CDW [27].

To answer the question whether the giant low-frequency peak can also be assigned to some phase phonon we compare temperature dependence of its intensity with that of the phase phonons (see Fig. 5). The latter is proportional to the square of the order parameter and reduces strongly upon approaching $T_p = 261$ K from below. Some residual intensity remains even at temperatures above T_p because of the short CDW order. From dashed line in Fig. 5 is shown the mean-field behavior of the square of the order parameter which is proportional to $(T_p - T)^{2\beta}$ with $\beta = 0.17$. The latter value of β is in good agreement with X-ray measurements [28]. In contrast to the phase phonon intensity, the integrated intensity (or, in the other words, oscillator strength) of the giant low-frequency peak slightly increases upon heating suggesting quite different origin of this vibration. Also, the resonant frequency of the peak displays a pronounced red shift upon heating in contrast to nearly temperature-independent frequencies of the high-frequency phonon structure.

The increase in the CT mode intensity shown in Fig. 5 can be naturally explained within our model. Indeed, as it is clear from Fig. 3 the integrated intensity of the CT mode as a function of the system parameters can be approximated as (see dashed line in Fig. 3)

$$I \simeq C_0 e^2 \left[\sqrt{\frac{2K_2 e^2 a^3}{Vb^3}}\right]^{-2.25} = C_0 e^{-0.25} \left[\sqrt{\frac{2K_2 \cdot a^3}{V \cdot b^3}}\right]^{-2.25}, \quad (6)$$

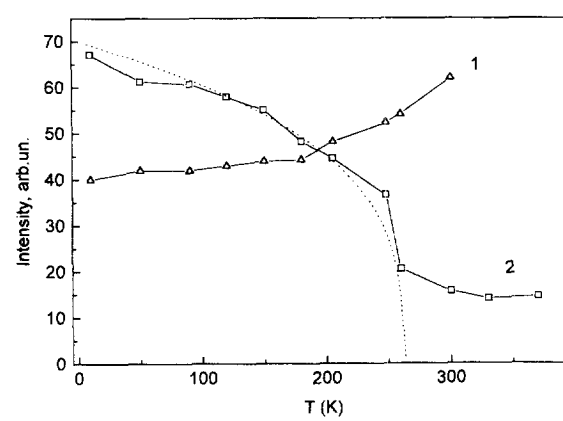

Fig. 5. Temperature dependences of the integrated intensities of the phase phonons and the CT mode at $\sim 38\ cm^{-1}$ (see Fig. 4).

where C_0 is constant and all the parameters as well except the particle charge.

The latter represents CDW amplitude and decreases upon approaching $T_p \simeq 261$ K from below. Due to short-range order the particle charge remains finite even at very high temperatures. Now, one can see that CT mode intensity increases upon the particle-charge decrease. To estimate the latter recall that the pseudogap value, describing the quasi-particle thermal excitation over the Peierls gap, decreases by factor 2 above the Peierls transition temperature T_p [29]. Using Eq. (6), one obtains about 20% increase in the CT mode intensity suggesting the particle charge to be decreased by factor 2 above T_p. It should be pointed out, that we suppose the Column-type interaction between CDW periods, although it is of much stronger distance (and probably charge) dependence. Therefore, the obtained estimation is very likely an estimation from below.

Note several features of the CT peak. Firstly, in contrast to the phase mode, its frequency does not depend on pinning (see Fig. 2). It also does not depend on the number of particles in the coherent CDW domain or, in the other words, on the effective mass of CDW condensate. The latter can explain why the corresponding frequency has nearly the same value in such different compounds as $K_{0.3}MoO_3$ and $(TaSe_4)_2I$ [13, 14].

3. Summary

We have presented a model and experimental investigation of vibrational spectrum of quasi-one-dimensional CDW conductor $(TaSe_4)_2I$. The microscopic mechanism accounting for the giant IR peak at frequencies about $\sim 40\,cm^{-1}$ in the $(TaSe_4)_2I$ and based on an assumption about dynamical charge transfer between adjacent CDW periods is proposed. The mechanism is consistent with the increase in the IR intensity of the $40\,cm^{-1}$ peak observed upon heating the $(TaSe_4)_2I$ crystal. Critical index of the Peierls transition order parameter has also been determined from the temperature dependence of the phase phonons intensity.

Acknowledgements

The work in Germany was supported by the European Communities under Contract No. CI1-0526-M(CD) and by the Deutsche Forschungsgemeinschaft. One of the authors (V.B.) gratefully acknowledges the support from Deutsche Forshungsgemeinschaft (DFG) of his visit in the Institut für Angewandte Physik Universität Karlsruhe. The work in Florida was supported by NSF Grant DMR–9403894. The work in Russia was supported by Russian Foundation of Fundamental Research under contract No. 96-02-18114a.

References

[1] S. Donovan, Y. Kim, B. Alavi, L. Degiorgi, G. Grüner, Solid. State. Commun. 75 (1990) 721.
[2] Y. Kim, L. Degiorgi, B. Alavi, G. Grüner, Sinth. Met. 41 (1991) 3959.
[3] L. Degiorgi, G. Grüner, Europhys. Lett.
[4] G. Grüner, Rev. Mod. Phys. 60 (1988) 1129.
[5] P. Monceau (Ed.), Electronic Properties of Inorganic Quasi-One-Dimensional Compounds, Parts 1 and 2.
[6] S. Kagoshima, H. Nagasawa, T. Sambongi, One-Dimensional Conductors, Springer, Berlin, 1988.
[7] M.B. Walker, Canad. J. Phys. 56 (1978) 127.
[8] G. Travaglini, P. Wachter, Phys. Rev. B 30 (1984) 1921.
[9] G. Travaglini, I. Mörke, P. Wachter, Solid. State. Commun. 45 (1983) 289.
[10] Tomoyuki Sekine, Taisaku Seino, Mitsuru Izumi, Etzuyuki Matsuura, Solid. State. Commun. 53 (1985) 767.
[11] M.S. Sherwin, A. Zettl, P.L. Richards, Phys. Rev. B 36 (1987) 12.
[12] T.W. Kim, D. Reagor, G. Grüner, Phys. Rev. B 40 (1989) 5372.
[13] T.W. Kim, S. Donovan, G. Grüner, A. Philipp, Phys. Rev. B 43 (1991) 6315.
[14] L. Degiorgi, B. Alavi, G. Mihaly, G. Grüner, Phys. Rev. B 44 (1991) 7808.
[15] L. Degiorgi, G. Grüner, Phys. Rev. B 44 (1991) 7820.
[16] Y.I. Frenkel, T. Kontorova, Zh. Eksp. Teor. Fiz. 8 (1938) 1340.
[17] M. Peyrard, S. Aubry, J. Phys. C 18 (1985) 4903.
[18] F.C. Frank, J.H. van der Merwe, Proc. Roy. Soc. London Ser. A 198 (1949) 205.
[19] F.C. Frank, J.H. van der Merwe, 198 (1949) 216.
[20] F.C. Frank, J.H. van der Merwe, 200 (1949) 125.
[21] R.K. Bullough, P.J. Caudrey (Eds.), Solitons, Springer, Berlin, 1980.
[22] P.J. Caudrey, J.C. Eilbeck, J.D. Gibbon, Nuovo Cimento 25 (1975) 497.

[23] V.M. Burlakov, M.A. Moskalenko, Pisma v Zh. Eksp. Teor. Fiz. 65 (1997) 750.
[24] M.E. Itkis, J.W. Brill, Phys. Rev. Lett. 72 (1994) 2049.
[25] M.J. Rice, Phys. Rev. Lett. 37 (1976) 36.
[26] M.J. Rice, Proc. Int. Conf. on Quasi One-Dimensional Conductors, Dubrovnik, 1978, Springer, Berlin, 1979.
[27] M.J. Rice, L. Pietronero, P. Bruesch, Solid. State. Commun. 21 (1977) 757.
[28] H. Fuhishita, M. Sato, S. Sato, S. Hoshino, J. Phys. C 18 (1985) 1105.
[29] D.C. Jonstone, J.P. Stokes, R.A. Klemm, J. Magn. Magn. Mater. 54 (1986) 1317.